

Complex evolutionary interactions in multiple populationsKaipeng Hu ¹, Pengyue Wang ¹, Junzhou He ¹, Matjaž Perc ^{2,3,4,5,6} and Lei Shi ^{1,7,*}¹*School of Statistics and Mathematics, Yunnan University of Finance and Economics, Kunming 650221, China*²*Faculty of Natural Sciences and Mathematics, University of Maribor, 2000 Maribor, Slovenia*³*Department of Medical Research, China Medical University Hospital, China Medical University, Taichung 404332, Taiwan*⁴*Alma Mater Europaea, 2000 Maribor, Slovenia*⁵*Complexity Science Hub Vienna, 1080 Vienna, Austria*⁶*Department of Physics, Kyung Hee University, 26 Kyungheedaero-ro, Dongdaemun-gu, Seoul, Republic of Korea*⁷*Interdisciplinary Research Institute of Data Science, Shanghai Lixin University of Accounting and Finance, Shanghai 201209, China*

(Received 1 August 2022; accepted 22 March 2023; published 12 April 2023)

In competitive settings that entail several populations, individuals often engage in intra- and interpopulation interactions that determine their fitness and evolutionary success. With this simple motivation, we here study a multipopulation model where individuals engage in group interactions within their own population and in pairwise interactions with individuals from different populations. We use the evolutionary public goods game and the prisoner's dilemma game to describe these group and pairwise interactions, respectively. We also take into account asymmetry in the extent to which group and pairwise interactions determine the fitness of individuals. We find that interactions across multiple populations reveal new mechanisms through which the evolution of cooperation can be promoted, but this depends on the level of interaction asymmetry. If inter- and intrapopulation interactions are symmetric, the sole presence of multiple populations promotes the evolution of cooperation. Asymmetry in the interactions can further promote cooperation at the expense of the coexistence of the competing strategies. An in-depth analysis of the spatiotemporal dynamics reveals loop-dominated structures and pattern formation that can explain the various evolutionary outcomes. Thus, complex evolutionary interactions in multiple populations reveal an intricate interplay between cooperation and coexistence, and they also open up the path toward further explorations of multipopulation games and biodiversity.

DOI: [10.1103/PhysRevE.107.044301](https://doi.org/10.1103/PhysRevE.107.044301)**I. INTRODUCTION**

Although competition has been proven to be a momentous law of species evolution and biodiversity, the guiding role of widespread collaborative behaviors in biological systems cannot be neglected [1–3]. In social animals and microbial communities, particularly, individuals may form alliances to adapt to harsh environments and competition [4,5]. Observable examples include vampire bats sharing blood meals with each other and emperor penguins huddling together for warmth [6]. However, a stable cooperative system does not imply spontaneous altruism of all members but a dynamic coexistence of the prosocial and the antisocial behaviors [7–10]. A typical example is the “fig-fig wasp” system, in which the fig wasps may dynamically choose whether to pollinate figs [11].

Evolutionary game theory has been confirmed to be a favorable mathematical tool for studying cooperation in dynamic biological systems. According to the conventional approaches, the interactions among individuals are mainly abstracted into two categories, one of which is pairwise interaction with only two agents, and the other is group-wise interaction with more than two participants. The most

representative models for pair and group interactions, are the prisoner's dilemma game [12–14] and the public goods game [15,16], respectively. Since all defection is the unique pure-strategy Nash equilibrium, there are many analogous properties between the prisoner's dilemma game and the public goods game. For example, cooperative behavior can be facilitated by cyclic dominance when voluntary participation is permitted, whether it in a prisoner's dilemma game or a public goods game [17–19]. Nonetheless, the public goods game is not exactly the multiplayer extension of the prisoner's dilemma game as more complex features may emerge in group interactions [20,21]. In addition, pool-based mechanisms, such as pool punishment [22–25], pool reward [26–28], and pool exclusion [29,30], make the dilemma of multiple participants irreplaceable.

Both interaction modes are important for explaining evolutionary cooperation, but they are not entirely incompatible, as individuals may choose to participate in paired or group games based on their preferences or circumstances [31]. Previous studies and empirical evidence highlight the important reality that in ecological and epidemiological systems, organisms may be involved in different patterns of interaction with multiple populations [32–34]. Typically, viruses, which mutate rapidly during propagation, interact variously with different variants over a considerable period of time [35]. Turning back to the perspective of biological game theory, it

*lshi@ynufe.edu.cn

is shown that neutral payoffs between populations cause individuals to oscillate between cooperation and defection [36]. In addition, environmental differences [37,38] in individuals may lead to different strengths of their interactions [39–42], which are rarely considered in evolutionary game theory. In particular, within a sociobiological community, the different tasks undertaken by individuals may affect the strength of interactions within and between populations.

Based on such a background, this paper develops an approach to study the competition and cooperation with multiple populations. Specifically, intra- and interspecific interactions are considered to be of different types, with individuals being allowed to participate in different numbers of pair and group games simultaneously, depending on their local environment. Furthermore, both symmetrical and asymmetrical situations are considered, where the symmetry (asymmetry) means that individual fitness is equally (unequally) dependent on games within and between populations. Through the simulations, we find that cooperation can be significantly improved with the introduction of additional populations. Moreover, asymmetry is proven to be a possible way to promote cooperation but at the expense of biodiversity.

In the remainder of this paper, we elaborate on the evolutionary multipopulation game models and explore the mechanisms of cooperative behavior in biological systems. Under Results, we present the results for the symmetric model first, followed by the results for the asymmetric model. The main phenomena and analyses are also described in this section. Ultimately, we conclude this article and discuss other complex interactions by comparing them with other related studies.

II. METHODS

The proposed evolutionary game is performed on a $L \times L$ lattice with periodic boundary and *von Neumann* neighbors (degree $k = 4$). Individuals from different populations are stochastically arranged on the nodes of the lattice and engaged in two types of interactions, namely the public goods game and the prisoner’s dilemma game. Specifically, the intrapopulation interaction is defined as the public goods game and interpopulation interaction as the prisoner’s dilemma game. Since opponents may belong to different populations, the focal player has the opportunity to participate in prisoner’s dilemma games and public goods games, simultaneously. In particular, one has to participate in $n = k + 1$ groups of public goods games when all of its opponents belong to the identical population as it. On the contrary, it plays k pairs of prisoner’s dilemma games when all of the opponents belong to another population. More generally, it plays $n = k_s + 1$ groups of public goods games, and $k - k_s$ pairs of prisoner’s dilemma games, where k_s is the number of opponents who belongs to the same population as it. Note that $k_s \geq 1$ indicates that the public goods game will not be organized within a single player.

In a group of the public goods game, cooperators devote $c = 1$ to the common pool, while defectors contribute nothing. The sum of the contributions is multiplied by a synergy factor r , then it is distributed equally to the participants. The payoffs of cooperators and defectors in a given group g can be

expressed as:

$$P_C^g = n_c r / n - c$$

$$P_D^g = n_c r / n,$$

where n_c denotes the number of cooperators in the group. Unlike the conventional setting, everyone has a fixed initial endowment $E = k + 1$ to guarantee non-negative cumulative payoffs even when participating in $k + 1$ groups of public goods game.

In the prisoner’s dilemma game, if two cooperators (defectors) meet, both receive $R(P)$; if a cooperator competes with a defector, then the cooperator (defector) receives $S(T)$. In this paper, the payoff matrix can be illustrated as:

	C	D
C	$R = 1 + u$	$S = 0$
D	$T = 1 + 2u$	$P = u$

where $0 < u < 1$, satisfied the essence of the prisoner’s dilemma game that $T > R > P > S$, and $2R > T + S$. What we must pay attention is that such a payoff matrix is adopted to ensure that participants have a non-negative return in the prisoner’s dilemma game.

By interacting with all its neighbors, player x derives a cumulative payoff P_x^{PGGs} from intrapopulation competitions, and another cumulative payoff P_x^{PDGs} from interpopulation competitions. In the symmetric interaction case, the participants in each population have the same intensity of interaction within and between populations, and then their fitness is equally dependent on the returns of public goods game and the prisoner’s dilemma game. Thus, player’s fitness is simply defined as $F_x = P_x^{PDGs} + P_x^{PGGs}$.

In the asymmetric interaction case, we analyze the evolutionary dynamics of cooperation with only two populations. Considering the different interaction strengths within and between populations, the fitness configurations for population A and B are constructed as $F_x = (1 - \alpha)P_x^{PGGs} + (1 + \alpha)P_x^{PDGs}$ and $(1 + \alpha)P_x^{PGGs} + (1 - \alpha)P_x^{PDGs}$, respectively. The parameter α takes values within the range $[0, 1]$ indicating the degree of asymmetry between populations. When only interpopulation interactions are considered, population A has an advantage over population B in fitness due to the introduced asymmetry, so we next simply name them as strong and weak populations, respectively.

Starting from states where cooperators and defectors (from all swarms) are randomly arranged on lattice nodes, a complete *Monte Carlo* (MC) step contains an average chance of all individuals to update their strategies and population attributions. For the strategy update, we selected the Fermi rule, one of the most popular and accepted approach in evolutionary game theory [43,44], as it facilitates the comparison of results. Specifically, an individual decides whether to imitate one of his random neighbors by the following probabilities:

$$\Gamma_{(s_y \rightarrow s_x)} = 1 / \{1 + \exp[(F_x - F_y) / K]\},$$

where x and y represent the random selection of adjacent players, $S_x(S_y)$ and $F_x(F_y)$ indicate their strategies and fitness. We fix $K = 0.5$ as the inverse of the chosen temperature to obtain comparable results with existing studies [45]. We

employ the size of linear systems ranging from $L = 400$ to 4000, in accordance with the proximity of the phase transition points [22,46,47]. To a certain extent, using a sufficiently large system size may enable us to guarantee the accuracy of an evolutionarily stable solution. Conversely, the final outcome of the evolution may be largely influenced by stochasticity. In addition, the quantitative results at the steady state are determined by the average of the last 5000 steps in 100 000 MC step simulations.

III. RESULTS

A. Symmetric populations

Before presenting the main results, we briefly analyze the evolutionary dynamics in a single population and therefore without interpopulation interaction (prisoner's dilemma game). In this case, each player engages in $k + 1 = 5$ groups of public goods games, and individuals are distinguished only by strategy. The model we proposed gives all individuals equivalent initial endowments, which is different from the traditional spatial public goods game. But it does not affect the evolutionary outcome of cooperation. Therefore, when the synergy factor r exceeds the group size, cooperators entirely dominate the system. Conversely, when it is below a threshold (about $r = 3.74$), all the cooperators die out [23].

We next discuss the representative outcome of two symmetric populations, defined as A and B, respectively. Just like the role of r in the public goods game, the parameter u unilaterally determines the strength of the prisoner's dilemma. Consequently, these two parameters jointly determine the evolutionary dynamics of cooperation in cases where both dilemmas are involved in this paper. In Fig. 1, we present the stationary cooperation frequency of the whole system in dependence on the parameter r and u . Not surprisingly, the cooperation frequency decreases with increasing dilemma strength [49,50]. Notably, an increase in the parameter r or decrease in u can significantly improve the cooperation rate. Compared to the case of a single population, collaborative behavior is more favorable when interpopulation competitions are permitted. From the perspective of the public goods game, the threshold at which cooperation emerges declines from about $r = 3.74$ to $r = 2.5$. When the reciprocity of the public goods game reaches another threshold (about $r = 4$), the increase in strength of the prisoner's dilemma does not lead to the extinction of the cooperators. Conversely, at the given parameter range in Fig. 1, no matter how weak the dilemma is, there is no full cooperation state.

The spatiotemporal dynamics animation in Ref. [48] reveals the intrinsic mechanism by which cooperation is facilitated in a system comprising two symmetric populations. Correspondingly, a typical snapshot in the stationary state and the evolutionary process of the frequencies of the strategies are presented in Fig. 2. Cooperators and defectors in the snapshot and the animation are colored in blue and red, while the shade of the colors indicate the population to which the player is affiliated. The frequency of strategies in Fig. 2(b) would adopt the same color scheme, and solid and dashed lines represent the case of populations A and B, respectively. In the left panel, some patches are circled, which express representa-

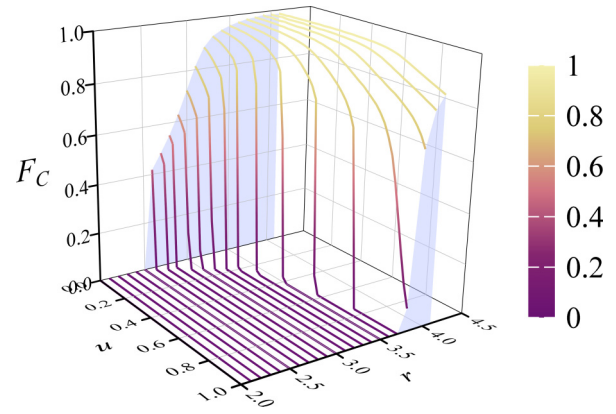


FIG. 1. The stationary cooperation frequency. Depicted above is the overall cooperation rate F_C consisting of two populations on the (u, r) plane. These results show that the introduction of an additional population, which enables inter- and intrapopulation interactions to coexist in the system, significantly enhances the cooperation rate.

tive features during evolutionary dynamics. The white circles marked “1,” “2,” and “3” show that cooperators from population A are surrounded by cooperators from population B, while the circles marked “4” and “5” show the opposite cases. These patches indicate that cooperators at the interface of different populations can invade each other. This is because the cooperators did not participate in the two games in the same amount, so they did not have exactly the same fitness. For a similar reason, defectors belonging to different populations can also invade each other.

Afterward, we explore another crucial characteristic of the system. As shown by the circled patches marked “6” and “7” in Fig. 2(a), a few defectors spirally attached in the gaps of large cooperation patches from populations A and B. The patch marked “6” highlights that D_A defectors invade the C_A cooperators, while the territory thus acquired is quickly occupied by the C_B cooperators. Similarly, the circled patch marked “7” indicates that the D_B defectors beat C_B cooperators but are beaten by C_A cooperators. In this case, a closed loop of $D_A \rightarrow C_A \rightarrow D_B \rightarrow C_B \rightarrow D_A$ appears in the system, which further leads to a dramatic improvement in cooperation. From the right panel of Fig. 2, the characteristics of closed-loop invasion are reflected. We can also find that the frequency of strategies does not converge over time but dominates cyclically within a certain range. Furthermore, the amplitude cooperation rate (the frequency of C_A and C_B) is markedly higher than defectors (the frequency of D_A and D_B). Since the direction of the mutual invasion of cooperators is unilaterally determined by the shape of the interface between the two populations, it does not lead to large fluctuations in cooperation frequencies. Therefore, the slight fluctuation in defector frequency induces a tremendous fluctuation in cooperation rates, and it is obvious that the loop invasion plays a more important role in the evolutionary dynamics than the mutual invasion of cooperators from different populations.

To get a clearer understanding of the above two dynamic characteristics, we show the evolutionary dynamics from a prepared initial state in Fig. 3. Such a special initial distribution of the strategies allows more kinds of interactions to

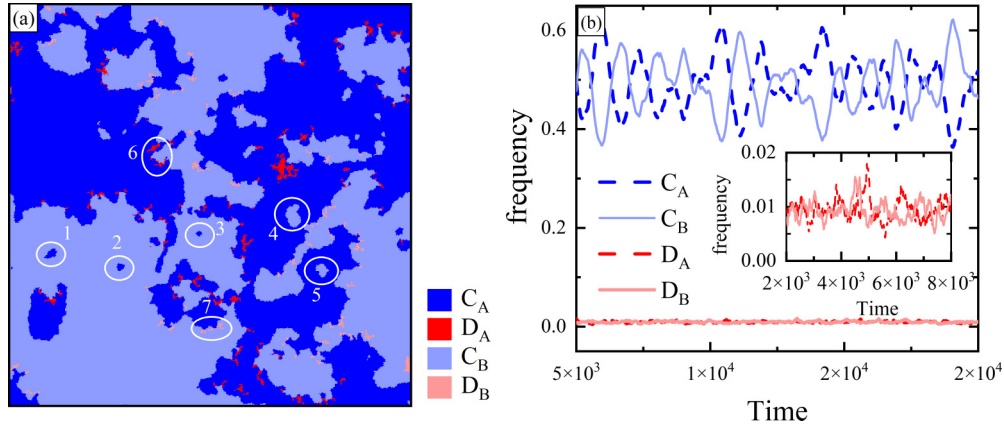


FIG. 2. (a) Typical snapshot of the stationary distribution of strategies consisting of two populations. Cooperators and defectors belonging to the symmetric populations are referred to here as A and B, which are depicted in bright (light) blue and bright (light) red, respectively. The circled patches reveal the core mechanism of evolutionary dynamics, and details can be observed in the animation [48]. In particular, the closed loop of $D_A \rightarrow C_A \rightarrow D_B \rightarrow C_B \rightarrow D_A$ is found to further promote the formation of spiral patches. (b) The evolutionary frequency of the four strategies corresponding to the left panel, and a built-in illustration scaling down the coordinates to observe the defection rate. The closed loop can be understood with the oscillating frequency of the four competing strategies. The results for both panels are obtained with $r = 3.8$, $u = 0.05$, and $L = 500$.

be visualized [22]. From the next panel, the bright (light) blue rapidly invades light (bright) red, while being slowly invaded by the bright (light) red. However, from the corresponding interfaces, one can see that the competition of cooperators (or defectors) between different populations appears to be more moderate. Although it can be found from Fig. 3 that the system undergoes drastic changes, the spatial distribution of policies is roughly bilaterally symmetric. It highlights the extremely slow rate at which cooperators from different populations invade each other. The subsequent evolutionary results show that the territories are cyclically occupied by different species and explain the oscillating spatial diffusion of the strategies. Similar spatiotemporal features of loop dominance can be further traced from previous ecological studies [32,51–53] that reveal important ways in which species interact in terms of pattern and diversity.

The above results for two symmetric populations are sufficiently representative that we do not extend the analysis of the spatiotemporal dynamics of more than two populations [36]. Nonetheless, it is still worth discussing how the number of populations affects the evolution of cooperative behavior. In Fig. 4, we present the stationary cooperation frequency of the whole system in dependence on the parameter u for population

numbers equal to 2, 3, and 4. Note that the results of the single population are not shown, because we adopt $r = 3.2$ below the cooperation threshold ($r = 3.8$) that cooperator cannot survive without interpopulation interactions. The results are concise, the stationary frequency of the cooperation increases with the number of symmetric populations. In addition, a larger population in a system allows cooperation to persist in stronger dilemmas.

B. Asymmetric populations

In biological systems, stronger individuals may need to defend against external enemies and therefore have greater strength of interpopulation interactions and less strength of intrapopulation interactions. Here we only explore a simple case where the two populations participating in the interactions are divided into the strong and the weak. Therefore, the strategy set contains C_S, C_W, D_S , and D_W , which represent strong cooperators, weak cooperators, strong defectors, and weak defectors, respectively. Based on the coupling rules of the fitness for strong and weak, the parameter α , which is used to control the degree of asymmetry between the two

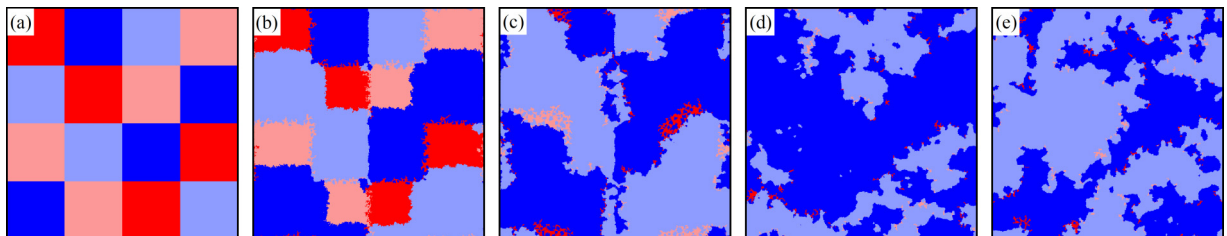


FIG. 3. Representative evolution of the four strategies from a prepared initial state. It can be observed that the interface between bright red (blue) and light red (blue) is very smooth and the mutual invasion of cooperators (defectors) from different populations is significantly slower than that between cooperators and defectors in the same population. It highlights that the dynamics of the closed loop dominates the evolution of the system. The results are obtained with $r = 3.8$, $u = 0.05$, and $L = 500$.

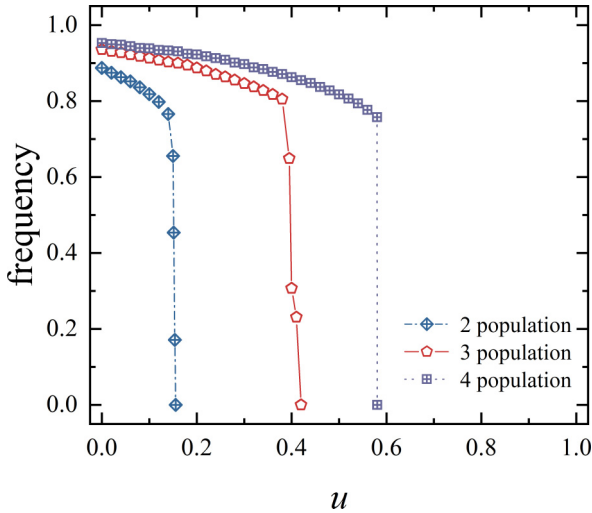


FIG. 4. The stationary frequency of cooperation in the whole system F_C in dependence on the parameter u as obtained for different numbers of populations. Note that the results of a single population are not shown because we adopt $r = 3.2$, which is below the cooperative threshold of $r = 3.8$ in the spatial public goods game. It implies that the additional populations considerably promote cooperation when interpopulation competitions are permitted.

populations, becomes an important factor affecting the evolutionary dynamics.

In Fig. 5, we illustrate the u - α phase diagram of the system as obtained for $r = 3.2$. In this case, the cooperators are survivable when competing symmetrically. The blue solid lines indicate the continuous phase transitions, while the red dashed lines indicate the discontinuous phase transitions. The phase diagram reveals several fundamental features associated with two asymmetric populations. First, it is shown that the phases containing cooperation form a triangle, which implies that

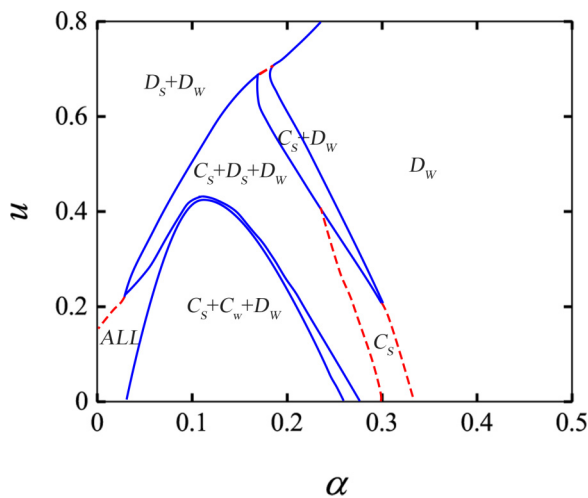


FIG. 5. The (u, α) phase diagram of the spatial game with two asymmetric populations as obtained for $r = 3.2$. The solid blue lines denote continuous phase transitions, while dashed red lines denote discontinuous phase transitions. The extremely narrow space between the triplets marked “ALL” refers to the $C_S + C_w + D_S + D_w$ phase.

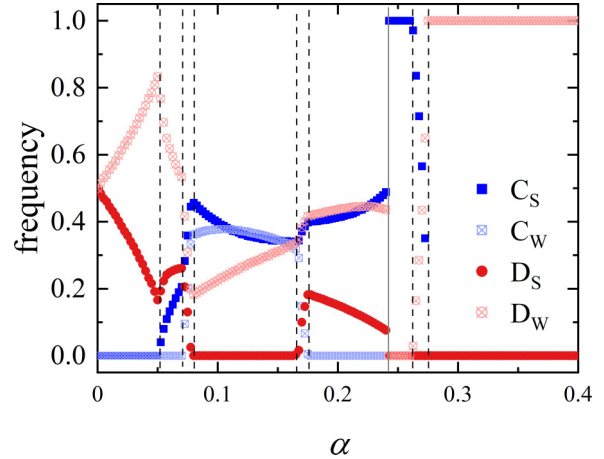


FIG. 6. The stationary frequency of the four strategies is dependent on the asymmetric factor α for $u = 0.33$ and $r = 3.2$. From this cross section, a series of phase transitions are reflected.

small values of u and moderate values of α are conducive to cooperators’ survival. In the triangle region, the C_S is always viable, and the $C_S + C_w + D_w$ and $C_S + D_S + D_w$ phases occupy the most area. Especially, the $C_S + C_w + D_w$ phase prevails when u is low, while the $C_S + D_S + D_w$ phase is dominant when u is high. Between the two triplets, there is a narrow inverted U-shaped phase, labeled “ALL,” indicating that the four strategies coexist in the system. Moreover, there is an important discontinuous phase transition process associated with the “ALL” phase, namely the system from the $D_S + D_w$ phase jumps into the $C_S + C_w + D_S + D_w$ phase with the decrease of u . The same phenomenon can also be observed in the results of symmetric interactions, which explain that biodiversity is only well maintained when the population is (asymptotically) symmetric. In that case, the dynamics of cooperation are mainly driven by the cyclic dominance of the four strategies, and once the closed loop is broken, all cooperators die out from the system simultaneously.

Interestingly, a full cooperation (C_S) phase appears when the degree of asymmetry is further increased, suggesting that asymmetry among populations may be the reason for promoting cooperation. The associated two discontinuous phase transitions include the $C_S + D_S + D_w$ phase transforms into the complete C_S phase as well as the complete C_S phase to complete the D_w phase. The former illustrates the disintegration of the defense alliance, while the latter highlights the extinction of cooperation. In addition, when the value of u is relatively large, the full C_S change into the $C_S + D_w$ phase through continuous phase transitions. It is surprising that the $C_S + D_w$ phase refers to a typical asymmetric interaction pattern in biological systems and is abstracted as a “box pigs” game [54,55].

In Fig. 6, we show the typical cross section of the phase diagram when $u = 0.33$. It can be observed that the system starts from a $D_S + D_w$ phase with an equal proportion of both strategies because the two populations are symmetric when $\alpha = 0$. With the increase of α , the density of D_w defector is getting higher, while the fraction of D_S defector is getting lower. Understandably, defectors from both populations hold

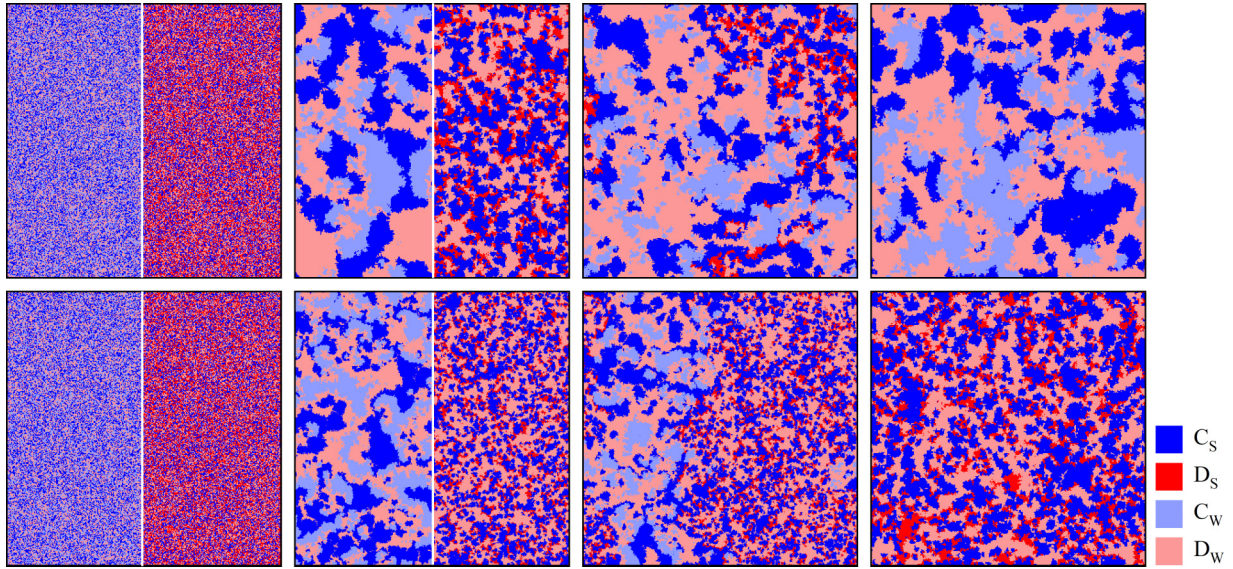


FIG. 7. Consecutive snapshots of the evolutionary system, as obtained for $u = 0.1$, $\alpha = 0.23$ (top row) and $u = 0.3$, $\alpha = 0.2$ (bottom row) from a prepared initial state. The cooperators and defectors from the strong (weak) population are colored in bright (light) blue and bright (light) red. During relaxation, the lattice is divided into two halves, and each half contains the strategies of one triplet. After the subsystem is evolutionarily stable (the typical features of the second column appear), the separating walls are removed, and the competition between the alliance starts. The top row shows that the $C_S + C_W + D_W$ triplet is dominant, while the bottom row shows that the $C_S + D_S + D_W$ triplet is dominant. Other parameters are $r = 3.2$ and $L = 600$.

the same payoff when all cooperators disappear from the system, and the coupling rule gives a higher degree of fitness to the weak than to the strong, as the α value increases. With the further increase of α , C_S cooperators join the fray, and the system forms into a $C_S + D_S + D_W$ defensive alliance, and the cooperation rate is monotonically promoted under this solution. Once again, it emphasizes that asymmetry facilitates cooperation. Next, the reentrant phase transitions involving a series of continuous transitions between triplets and quadruplets are clearly illustrated. Specifically, as α increases, the system starts from the $C_S + D_S + D_W$ phase, across the “ALL” phase (twice) and the $C_S + C_W + D_W$ phase, and finally returns to the starting state. What this process expresses is not a simple competition between C_W and D_S , but a war between different triple alliances. After that, the system unexpectedly jumps into the complete C_S state, this discontinuous phase transition reveals that the alliance of $C_S + D_S + D_W$ is broken by the increased asymmetry. With the continuous increase of α , D_W defectors coexist with C_S cooperators and finally achieve full dominance of D_W . Although the case of larger values of α is not shown, we can understand that excessive asymmetry is only profitable to the evolution of D_W defectors.

We subsequently explain the mechanisms of these solutions and relevant phase transitions from the spatiotemporal dynamic characteristics. In Fig. 7, the cooperators and defectors are colored in blue and red, while the shades are used to distinguish the strong and weak populations. During relaxation, the lattice is divided into two halves, and each half contains the strategies of one triplet. Both rows of the snapshots depict the evolution process of the four strategies from the separate subsystems to the merged system. This particular simulation method helps to explain the formation of

alliances and the competition among them [56,57]. From the corresponding animations in [58,59], the disordered strategies rapidly evolve into spiral patches. The static snapshots in the first two columns of Fig. 7 briefly describe this process, and this loop invasion is the most typical feature of the evolutionary rock-paper-scissors game [60–63]. Specifically, from the left part of the second column, the spiral plaques imply that the C_W cooperator dominates the C_S cooperator, but is dominated by the D_W defector; while from the right part, the D_S defector beats the C_S cooperator but are beaten by D_W defector. The triplets on both sides thus form corresponding closed loops, namely $C_S \rightarrow C_W \rightarrow D_W \rightarrow C_S$ in the left half and $D_W \rightarrow D_S \rightarrow C_S \rightarrow D_W$ in the right part. Although the evolutionary snapshots of the $C_S + C_W + D_S + D_W$ phase are not shown, it is understandable that both loops coexist in the “ALL” phase. What is more, the top row reveals the dynamics when the $C_S + C_W + D_W$ triplet is more aggressive, while the bottom row reveals the opposite case. In Fig. 8, we present the evolutionary dynamics of the four strategies, where D_S (C_W) is absent in the left (right) panel. Thus, the initial proportions of the strategies in both panels are $1/3$. It can be seen that the amplitude of the strategy oscillation in the $C_S + C_W + D_W$ triplet is greater than that of $C_S + D_S + D_W$. Combined with the size of the triplets shown in Fig. 7 and the result in Ref. [64], we conclude that in “oscillatory systems,” the larger spiral plaques and amplitudes of the evolutionary frequency of the strategies reveal the slower strategies transition rate.

In Fig. 9, we explain the mechanism of the full C_S phase through the consecutive snapshots. In the initial state, the four strategies are randomly arranged on the nodes of the lattice. In general, individuals gain significantly more from the public goods game than from the prisoner’s dilemma game,

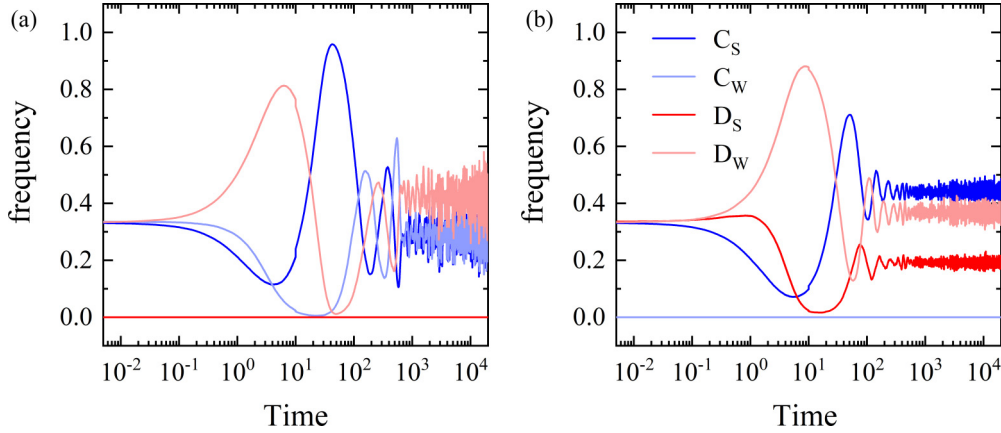


FIG. 8. Time evolution of the strategy frequency from a prepared initial state, and both panels adopt the same parameters $r = 3.2$, $u = 0.1$, and $\alpha = 0.23$. (a) The evolution in the absence of D_S defectors, and (b) the evolution in the absence of C_W cooperators. The results are obtained with $L = 400$.

as can be calculated from the payoffs. In a highly asymmetric situation, the weak population are more competitive than the strong population. For these reasons, only a few bright blues and bright blues remain in the sea of light blues and light reds in Fig. 9(b). Considering the Nash equilibrium of the public goods game, the defector is always at the advantage of the same population competition, thus the C_W cooperators are quickly expelled from the system by the D_W defectors. Then, there are only the C_S cooperators and the D_W defectors in the system, and the negative feedback mechanism induced by network reciprocity enables the further expansion of the C_S clusters until the eventual full domination. Note that the last panel of Fig. 9 does not represent the final state of the evolution, but the consequence and the other details of the evolutionary dynamics can be observed in Fig. 10(b). In addition, among the three panels of Fig. 10, the frequency of C_S decreases dramatically at the beginning but slows down

after dropping to a very low level. The reason is that the small C_S clusters are formed to resist the invasions, as can be found in Fig. 9. In the three panels, both the C_W and D_S are not competitive enough to survive and are eliminated the fastest. In the final stage of competition between the C_S and D_W , different results are reflected, namely the $C_S + D_W$ phase, the full C_S phase, and the full D_W phase, respectively.

Considering that the main conclusions in the above asymmetric populations are based on $r = 3.2$. In such a situation, cooperators and defectors are survivable even in symmetric interactions. To thoroughly understand the influence of asymmetry, we finally explore the evolutionary dynamics when $r = 2.4$ (the cooperation threshold of symmetric interaction is $r = 2.5$). In Fig. 11, it can be seen that cooperation persists in three different forms, namely $C_S + D_S + D_W$, $C_S + D_W$, as well as full C_S phase. Although the huge strength of the dilemmas, cooperation can be sustained by asymmetric interaction. However, there are fewer ways for strategies to coexist, such as the disappearance of the $C_S + C_W + D_W$ and $C_S + C_W + D_S + D_W$ phases. In addition, the phase diagram is very similar to the situation in Fig. 5 when larger values of u are embraced. It implies that the increase both in the intra- and interpopulation competition intensity results in a similar phenomenon in the biological system.

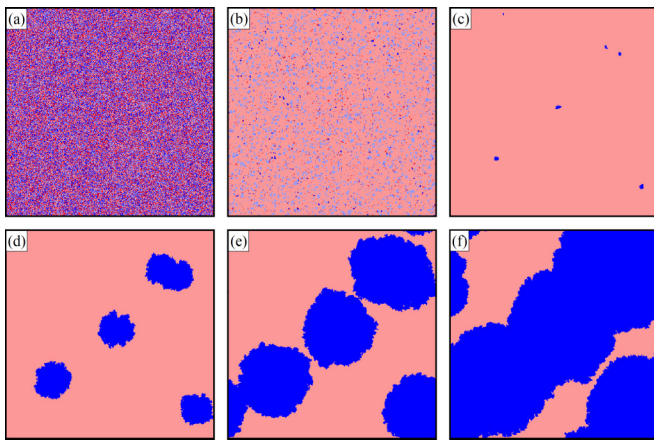


FIG. 9. Consecutive snapshots of the evolutionary system from a random state, as obtained for $r = 3.2$, $u = 0.1$, and $\alpha = 0.31$. The cooperators and defectors from the strong (weak) population are colored in bright (light) blue and bright (light) red. From (a) to (f), it explains the evolution of C_S phase dominance. The size of the adopted square lattice is 400×400 .

IV. DISCUSSION

Pairwise and groupwise interactions are the primary abstractions for individual competition. Based on these approaches, phenomena such as cooperation, invasion, ecological stability, and biodiversity are explained. From the perspective of cooperation and evolutionary games, only a very small amount of literature considers the coexistence of both competition modes [31]. However, the analysis of such complex interactions is necessary, and this paper provides a different framework to investigate it. Different from the basic setting in previous studies [65–68], we make it possible for one to participate in different types of interactions simultaneously.

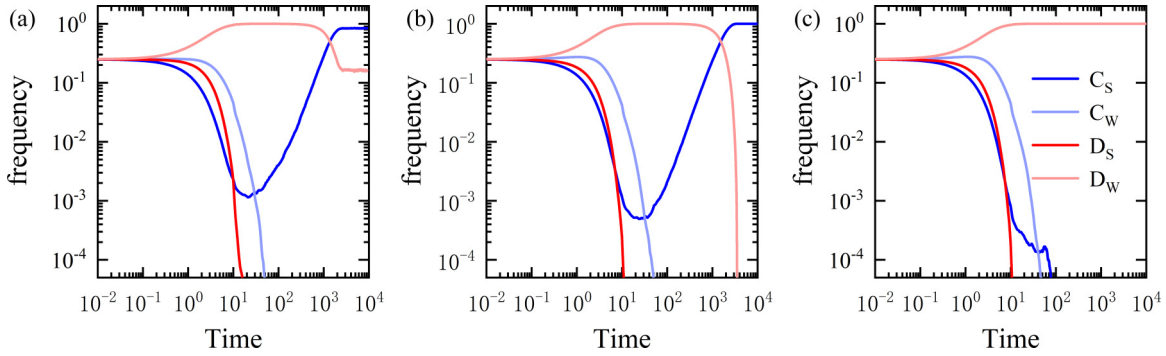


FIG. 10. Time evolution of the proportion of the four strategies from a random initial state for $r = 3.2$. Panel (a) is obtained for $u = 0.33$ and $\alpha = 0.265$; panel (b) is obtained for $u = 0.1$ and $\alpha = 0.31$; panel (c) is obtained for $u = 0.1$, and $\alpha = 0.32$. The three panels explain the formation of the $C_S + D_W$, C_S , and D_W phase. The results are obtained with $L = 1000$.

Specifically, players on the nodes of the network are divided into two or even more populations, the intrapopulation interactions are defined as groups of public goods games, while the interpopulation interactions are defined as pairs of prisoner’s dilemma games. Both symmetric and asymmetric interactions are taken into account in this paper. In the symmetric competition model, individuals from each population have the same competitiveness (consistent fitness structure). We find that the introduction of additional populations and the interpopulation competitions is beneficial to the maintenance of cooperation and biodiversity. From the spatiotemporal features, the cooperator from one population dominates the defector from another population, while the defector dominates the cooperator in intrapopulation interactions. In this way, a closed loop appears in the system, and cooperation and biodiversity are maintained by such dynamics.

However, the assumption of fully symmetric interaction is difficult to achieve in biological systems [69–71]; therefore, it is necessary to explore the asymmetric case. Specifically,

individuals are categorized as strong or weak depending on their degree of dependence on either inter- and intrapopulation interactions. This asymmetry between the populations can be quantified by the difference in this degree of dependence. We found that a moderate level of asymmetry is optimal for promoting the evolution of cooperation between the two populations. However, increasing the asymmetry between populations leads to a reduction in the number of coexistent strategy tuples in the system. This suggests that high levels of asymmetry can have a significantly negative impact on biodiversity, ultimately even leading to its destruction.

In summary, this paper analyzed the evolutionary dynamics of cooperation and biodiversity and the effect of the asymmetry in multipopulation systems. It is noteworthy that the setting of simply introducing the two game models mentioned above as the interactions within and between populations is lacking in general applicability. In particular, both share essentially the same dilemma structure [72], and there remain several classical models of pairwise interactions that have not been applied to our work. It is foreseeable that the cooperation can be further improved when the interaction models are transformed into weaker dilemmas, such as the Snowdrift game and the Harmony game. We would like to address these issues by using dilemma strength theory [50,73], which constructs intrinsic connections between different pairwise game models and reveals the generality of social dilemmas. Furthermore, how to construct a universal dilemma scale related to population size becomes another important part of our future work.

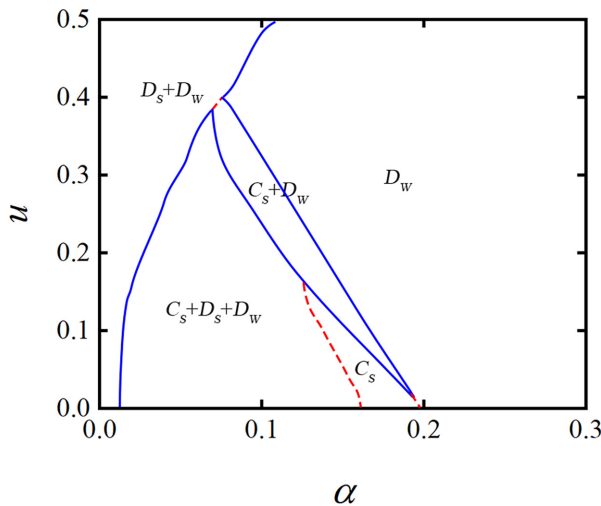


FIG. 11. u - α phase diagram of the spatial game with two asymmetric populations, as for $r = 2.4$. The solid blue lines denote continuous phase transitions, while dashed red lines denote discontinuous phase transitions.

ACKNOWLEDGMENTS

This research was supported by the National Natural Science Foundation of China (Grant No. 11931015) to L.S. We also acknowledge support from the China Scholarship Council (scholarship No. 202108530156) to K.H., the National Natural Science Foundation of China (Grants No. 32160239 and No. 31560134) and the Provincial high-level talent special support plan of Yunnan (YNWR-QNBJ-2019-233) to J.H., and the Slovenian Research Agency (Javna agencija za raziskovalno dejavnost RS) (Grants No. P1-0403, No. J1-2457, No. J4-9302, and No. J1-9112) to M.P.

- [1] A. S. Griffin, S. A. West, and A. Buckling, *Nature (London)* **430**, 1024 (2004).
- [2] S. A. West, I. Pen, and A. S. Griffin, *Science* **296**, 72 (2002).
- [3] E. Fehr and U. Fischbacher, *Econ. J.* **112**, C1 (2002).
- [4] R. J. Arend, *Strateg. Manage. J.* **30**, 371 (2009).
- [5] Y. Mao, X. Xu, Z. Rong, and Z.-X. Wu, *Europhys. Lett.* **122**, 50005 (2018).
- [6] G. Roberts, *Curr. Biol.* **30**, R307 (2020).
- [7] M. Perc, *Phys. Rev. E* **84**, 037102 (2011).
- [8] F. P. Santos, F. C. Santos, and J. M. Pacheco, *Nature (London)* **555**, 242 (2018).
- [9] S. Gavrillets and P. J. Richerson, *Proc. Natl. Acad. Sci. USA* **114**, 6068 (2017).
- [10] D. G. Rand and M. A. Nowak, *Nat. Commun.* **2**, 434 (2011).
- [11] R. W. Wang, L. Shi, S. M. Ai, and Q. Zheng, *J. Anim. Ecol.* **77**, 616 (2008).
- [12] M. Nowak and K. Sigmund, *Nature (London)* **364**, 56 (1993).
- [13] A. Yamauchi, J. Tanimoto, and A. Hagishima, *BioSystems* **102**, 82 (2010).
- [14] P. S. Park, M. A. Nowak, and C. Hilbe, *Nat. Commun.* **13**, 737 (2022).
- [15] A. Tavoni, A. Dannenberg, G. Kallis, and A. Löschel, *Proc. Natl. Acad. Sci. USA* **108**, 11825 (2011).
- [16] X. Chen, A. Szolnoki, and M. Perc, *Phys. Rev. E* **92**, 012819 (2015).
- [17] G. Szabó and J. Vukov, *Phys. Rev. E* **69**, 036107 (2004).
- [18] C. Hauert, S. De Monte, J. Hofbauer, and K. Sigmund, *Science* **296**, 1129 (2002).
- [19] D. Semmann, H.-J. Krambeck, and M. Milinski, *Nature (London)* **425**, 390 (2003).
- [20] M. Perc, J. Gómez-Gardenes, A. Szolnoki, L. M. Floría, and Y. Moreno, *J. R. Soc. Interface* **10**, 20120997 (2013).
- [21] A. Szolnoki, M. Mobilia, L.-L. Jiang, B. Szczesny, A. M. Rucklidge, and M. Perc, *J. R. Soc. Interface* **11**, 20140735 (2014).
- [22] A. Szolnoki and M. Perc, *Phys. Rev. X* **7**, 041027 (2017).
- [23] M. Perc, *Eur. J. Phys.* **38**, 045801 (2017).
- [24] Y. Fang, T. P. Benko, M. Perc, H. Xu, and Q. Tan, *Proc. R. Soc. A* **475**, 20190349 (2019).
- [25] A. Szolnoki and M. Perc, *Proc. R. Soc. B.* **282**, 20151975 (2015).
- [26] T. Sasaki and T. Unemi, *J. Theor. Biol.* **287**, 109 (2011).
- [27] T. Sasaki and S. Uchida, *Biol. Lett.* **10**, 20130903 (2014).
- [28] A. Szolnoki and M. Perc, *Europhys. Lett.* **92**, 38003 (2010).
- [29] L. Liu, X. Chen, and M. Perc, *Nonlinear Dyn.* **97**, 749 (2019).
- [30] L. Liu, S. Wang, X. Chen, and M. Perc, *Chaos* **28**, 103105 (2018).
- [31] A. Szolnoki and X. Chen, *Sci. Rep.* **11**, 12101 (2021).
- [32] M. B. Cronhjort, *Origins Life Evol. Biosphere* **25**, 227 (1995).
- [33] I. Scheuring, T. Czárán, P. Szabó, G. Károlyi, and Z. Toroczka, *Origins Life Evol. Biosphere* **33**, 319 (2003).
- [34] M. B. Cronhjort and C. Blomberg, *J. Theor. Biol.* **169**, 31 (1994).
- [35] D. H. Barouch, *N. Engl. J. Med.* **387**, 1011 (2022).
- [36] A. Szolnoki and M. Perc, *New J. Phys.* **20**, 013031 (2018).
- [37] C. Hilbe, Š. Šimsa, K. Chatterjee, and M. A. Nowak, *Nature (London)* **559**, 246 (2018).
- [38] A. R. Tilman, J. B. Plotkin, and E. Akçay, *Nat. Commun.* **11**, 915 (2020).
- [39] R. Wang, Z. Sun, L. Zhang, N. Yang, L. Feng, W. Bai, D. Zhang, Q. Wang, J. B. Evers, Y. Liu *et al.*, *Field Crops Res.* **253**, 107819 (2020).
- [40] R. L. Kordas, C. D. Harley, and M. I. O'Connor, *J. Exp. Mar. Biol. Ecol.* **400**, 218 (2011).
- [41] J. I. Griffiths, D. Z. Childs, R. D. Bassar, T. Coulson, D. N. Reznick, and M. Rees, *Proc. Natl. Acad. Sci. USA* **117**, 17068 (2020).
- [42] J. Davenport and W. Lowe, *J. Zool.* **298**, 46 (2016).
- [43] G. Szabó and C. Töke, *Phys. Rev. E* **58**, 69 (1998).
- [44] A. Szolnoki and M. Perc, *Phys. Rev. E* **87**, 054801 (2013).
- [45] M. Duh, M. Gosak, and M. Perc, *Phys. Rev. E* **102**, 032310 (2020).
- [46] H. Hinrichsen, *Adv. Phys.* **49**, 815 (2000).
- [47] G. Ódor, *Rev. Mod. Phys.* **76**, 663 (2004).
- [48] K. Hu (2022), https://figshare.com/articles/media/symmetric_mp4/19606957.
- [49] Z. Wang, S. Kokubo, M. Jusup, and J. Tanimoto, *Phys. Life Rev.* **14**, 1 (2015).
- [50] H. Ito and J. Tanimoto, *R. Soc. Open Sci.* **5**, 181085 (2018).
- [51] M. C. Boerlijst and P. Hogeweg, *Physica D* **48**, 17 (1991).
- [52] P.-J. Kim and H. Jeong, *Physica D* **203**, 88 (2005).
- [53] M. B. Cronhjort and C. Blomberg, *Physica D* **101**, 289 (1997).
- [54] Y. Wang, X. Wang, D. Ren, Y. Ma, and C. Wang, *Phys. Rev. E* **103**, 032414 (2021).
- [55] D. Jiang, Y. Shao, and X. Zhu, *Games Rev.* **2**, 1 (2016).
- [56] A. Szolnoki and M. Perc, *Europhys. Lett.* **110**, 38003 (2015).
- [57] A. Szolnoki and M. Perc, *New J. Phys.* **18**, 083021 (2016).
- [58] K. Hu (2022), https://figshare.com/articles/media/The_evolution_of-Cs_Cw_Dw_triplets_between_asymmetrical_populations_mp4/19606975.
- [59] K. Hu (2022), https://figshare.com/articles/media/The_evolution_of-Cs_Ds_Ds_triplets_mp4/19606984.
- [60] J. Menezes, *Phys. Rev. E* **103**, 052216 (2021).
- [61] D. F. P. Toupo and S. H. Strogatz, *Phys. Rev. E* **91**, 052907 (2015).
- [62] S. L. Jackrel, K. C. Schmidt, B. J. Cardinale, and V. J. Denef, *mBio* **11**, e02657-19 (2020).
- [63] T. Reichenbach, M. Mobilia, and E. Frey, *Nature (London)* **448**, 1046 (2007).
- [64] K. Hu, H. Guo, R. Yang, and L. Shi, *Europhys. Lett.* **128**, 28002 (2020).
- [65] W. Huang, C. Hauert, and A. Traulsen, *Proc. Natl. Acad. Sci. USA* **112**, 9064 (2015).
- [66] L. Attia and M. Olliu-Barton, *Proc. Natl. Acad. Sci. USA* **116**, 26435 (2019).
- [67] S. Huck, P. Jehiel, and T. Rutter, *Game Econ. Behav.* **71**, 351 (2011).
- [68] X. Li, H. Wang, G. Hao, and C. Xia, *Phys. Lett. A* **384**, 126414 (2020).
- [69] O. P. Hauser, C. Hilbe, K. Chatterjee, and M. A. Nowak, *Nature (London)* **572**, 524 (2019).
- [70] A. McAvoy and C. Hauert, *PLoS Comput. Biol.* **11**, e1004349 (2015).
- [71] R. Wang, J. He, Y. Wang, L. Shi, and Y. Li, *Sci. China Life Sci.* **53**, 1041 (2010).
- [72] J. Tanimoto, *Phys. Rev. E* **87**, 062136 (2013).
- [73] J. Tanimoto and H. Sagara, *BioSystems* **90**, 105 (2007).